RESEARCH ARTICLE

# Calculation of Switching Overvoltage for the Case of a Bolted Three-Phase Short Circuit on a Medium-Voltage Feeder with Connected Induction and/or Synchronous Generators

**Vladica Mijailović**[1,*] **and Aleksandar Ranković**[1]

[1] Faculty of Technical Sciences Čačak, University of Kragujevac, Čačak 32000, Serbia

## Abstract

**This paper presents a procedure for calculating switching overvoltage on the main circuit breaker of a medium-voltage (MV) cable feeder, to which induction and/or synchronous generators are connected, during a three-phase short circuit. When a fault occurs, the feeder is disconnected by the circuit breaker located at its beginning. After the set operating time of the relay protection, since islanded operation is not permitted, the connected distributed generators will also be disconnected. It is shown that, during the period when the network is disconnected while the generators remain connected, the overvoltage factor reaches values between 2.2 and 2.5, depending on the types of generators and the location of points of common coupling. The individual transient responses of the distribution network and the mentioned types of distributed generators differ significantly. Using the superposition theorem, the calculation of switching overvoltage is demonstrated with elementary computer assistance.**

**Keywords**: distribution network, induction generator, superposition, switching overvoltage, synchronous generator.

## 1 List of symbols and abbreviations

### 1.1 Symbols

$d$, Distance (km); $e$, Instantaneous electromotive force of the equivalent voltage source (kV); $I$, Current (kA); $i$, Instantaneous current (kA); $j$, Imaginary unit (-); $L$, Inductance (H); $l_{\text{feeder}}$, Feeder series-inductance per unit length (H/km); $m$, Transformation ratio (kV/kV); $R$, $r$, Resistance ($\Omega$, p.u.); $r_{\text{feeder}}$, Feeder series-resistance per unit length ($\Omega$/km); $S$, Apparent power (MVA); $s$, Slip (p.u.); $S''_N$, Sub-transient short-circuit power of the medium voltage distribution network (MVA); $T$, Time constant ($s$); $t$, Time ($s$); $U$, Voltage (kV); $V$, Voltage (kV); $X$, $x$, Reactance ($\Omega$, p.u.); $Z$, Impedance ($\Omega$); $\alpha_0$, Initial phase angle of the pre-fault voltage, i.e. phase angle corresponding to the three-phase voltage magnitude at $t = 0$ s (rad); $\varphi$, Phase angle of current with respect to voltage (rad); $\sigma$, Total leakage factor (p.u.).

**Submitted:** 08 December 2025
**Accepted:** 19 December 2025
**Published:** 29 December 2025

**Vol.** 1, **No.** 2, 2025.
10.62762/TEPNS.2025.181085

***Corresponding author:**
✉ Vladica Mijailović
vladica.mijailovic@ftn.kg.ac.rs

**Citation**
Mijailovic, V., & Ranković, A. (2025). Calculation of Switching Overvoltage for the Case of a Bolted Three-Phase Short Circuit on a Medium-Voltage Feeder with Connected Induction and/or Synchronous Generators. *ICCK Transactions on Electric Power Networks and Systems*, 1(2), 82–92.

### 1.2 Superscripts

′, Transient parameter; ″, Sub-transient parameter.

### 1.3 Subscripts

0, Initial or pre-fault value; 1, Point that corresponds to the terminals of the induction or synchronous generator; $a$, Aperiodic constant; $AB$, $AC$, $AF$, Parameter that corresponds to the circuit between the point A to another point; $AB$, $BC$, $CF$, Parameter of the circuit between two points; $d$, Direct-axis short-circuit parameter; $e$, Equivalent circuit parameter; $F$, Variable that corresponds to the circuit between the points C and F; $feeder$, Parameter of the feeder; $IG$, Induction generator's parameter or variable; $B-IG$, Induction generator connected at the point B; $IGT$, Parameter of the induction generator step-up transformer; $L$, Variable that corresponds to the circuit between the points B and C; $left$, $right$, Parameter or variable of the universal equivalent circuit on the left or right side from the distributed generator or medium voltage distribution network, respectively; $m$, Magnetising circuit parameter; $max$, Maximum value; $N$, Medium voltage distribution network's parameter or variable; $n$, Rated value; $r$, Rotor circuit parameter; $s$, Stator circuit parameter; $sc$, Short-circuit value; $SG$, Synchronous generator's parameter or variable; $B-SG$, Synchronous generator connected at the point B; $SGT$, Parameter of the synchronous generator step-up transformer; $source$, Parameter or variable of the universal equivalent circuit, in the branch representing the inputs; $x$, where $x=IG$, $x=N$ or $x=SG$, Variable that corresponds to the input; $\sigma$, Parameter that corresponds to the leakage flux.

### 1.4 Abbreviations

DG, Distributed generator; IG, Induction generator; MV, Medium voltage; SC, Short-circuit; SG, Synchronous generator.

## 2 Introduction

The most frequent fault in an electric power system (EPS) is a single-phase earth fault. If the fault occurs at the voltage peak, the overvoltage factor may reach values of up to 2.7 [1]. During the clearing of a three-phase fault, the overvoltage factor may also attain high value. For instance, in a passive electrical distribution network 10 kV, the overvoltage factor at the main circuit breaker, in the case of a busbar three-phase short circuit, is 1.997 [1].

There is not much available literature addressing the issue of switching overvoltages in active distribution networks. The over-voltage issue in low voltage distribution networks with high penetration of PVs is analyzed in [2]. A two-level voltage control methodology is proposed to deal with the over-voltage problem. The paper [3] reviews technical and operational barriers such as voltage fluctuations, congestion, and intermittency in RES-dominated grids. A novel three-layered implementation framework is proposed- comprising component, service, and regulatory layers- that unifies device-level technologies, grid services, and policy instruments into one coordinated roadmap. In power systems, single-phase earth faults are the most common type of fault. When a three-phase four-wire system supplied by an ungrounded synchronous generator is subjected to SLG faults, the unfaulted phases are expected to exhibit significant ground-fault over-voltage (GFOV). Mitigation of this is via effective grounding, as described in IEEE Std 62.92.2. However, for inverter-based resources (IBRs), the physical mechanism that leads to GFOV in synchronous machines is not present. The paper [4] investigates whether GFOV is a problem in IBRs, and whether conventional mitigation requirements, such as providing a grounding transformer (GTF), are suitable for IBR installations. An overvoltage adjustment strategy based on integrated voltage sensitivity in active distribution networks, focusing on the impact of photovoltaic energy sources on voltage regulation is discussed in [5]. In [6], a new method was introduced and evaluated to address the decline in power quality in distribution networks. Unlike previous studies, this approach considered random fluctuations in both individual loads and distributed generators over time focusing on improving the grid performance variables such as voltage profile index and power losses. The research paper [7] presents the impact of voltage rise effect and reverse power flow constraint in power systems with a high concentration of renewable distributed generators (RDG). The analysis is conducted on a sample distribution network (DN), i.e., IEEE 13-bus test system, with RDG penetration by considering the most critical scenario such as low power demand in DN and a peak power injection by RDG. For studying the impact of voltage rise and reverse power flow, a mathematical model of a DN integrating RDG is developed. The study [8] conducts a comprehensive evaluation, encompassing both steady-state and transient behaviours, leading to a holistic assessment of a real-world biogas generation system integrated into a medium-voltage network.

The key contributions of this study include identifying the effects of distributed generation systems (DGSs) on short-circuit currents, protection coordination, and defining voltage levels that briefly exceed the CBEMA quality curve. Ref. [9–16] focuses on the behavior of inductive, resistive, solid-state, and superconducting FCLs, including their transient response during fault interruption, their dynamic impedance characteristics, and their ability to reduce switching overvoltages.

This paper proposes a methodology for calculating overvoltages in an active distribution network, in which distributed energy resources of different types are connected to the feeder, under the condition of a three-phase short circuit. The calculation is performed for a fault occurring at the most unfavorable moment, while taking into account the following two facts:

- Circuit breakers interrupt the current at the instant when it reaches zero;
- On a feeder with distributed power plants connected, the fault currents contributed by the generators do not reach their peak values at the same time as the fault current supplied from the grid [1, 17–20].

The analyses presented in this paper are conducted for a section of an active distribution network of nominal voltage 10 kV, whose single-line diagram is shown in Figure 1, and for which the three-phase short-circuit current calculations were carried out in [17–20]. The feeder is supplied from the medium-voltage network, and different types of distributed generation (DG) may be connected at points $B$ and $C$ (if an induction generator, IG, is connected at point $B$, then a synchronous generator, SG, is connected at point $C$, and vice versa). The ratings of the IG and SG are selected such that, at no point and at no moment during normal operation, does an impermissible voltage rise occur, nor does any section of the feeder become overloaded. For a fault occurring at the most unfavorable instant, the times at which the corresponding fault currents reach their maximum values fall within the range from $t = 0.005s$ to $t = 0.011s$.

After the fault current is interrupted by the circuit breaker at point $A$, the circuit is separated into two segments in which independent transient phenomena take place: the transient process on the medium-voltage (MV) network side and the transient process on the feeder side.

The transient response on the network side is characterized by two components. The first is driven by the system excitation and is referred to as the forced (steady-state) component. The second represents the natural response of the circuit, decays over time, and is referred to as the transient (dc-offset) component [1].

The transient process on the feeder side is determined by the currents supplied from the connected distributed generators (DGs) toward the fault location. These currents must be interrupted by the circuit breakers associated with the DG units. Only after these currents are fully cleared does the system enter the transient phase governed by the residual electrostatic and electromagnetic energy stored in the feeder capacitances and inductances–a phenomenon also presents in conventional (passive) electrical distribution networks.

The current is interrupted at instant $t_p$. For $t < t_p$, the circuit breaker is closed and conducts the current $i(t)$. For $t \geq t_p$, the circuit breaker is open. The breaker is assumed to be ideal: when closed, its impedance is zero, and when open, its impedance instantaneously becomes infinite.

The voltage $u_{lr}(t)$ across the circuit breaker contacts after current interruption is given by

$$u_{lr}(t) = u_l(t) - u_r(t) \tag{1}$$

where $u_l(t)$ and $u_r(t)$ denote the voltages at node $l$ and node $r$ of the breaker, respectively [1].

The voltage difference $u_{lr}(t)$ that arises across the breaker terminals immediately after current interruption is defined as the transient recovery voltage (TRV) [1]. In TRV calculations, circuit breakers are commonly represented by idealized models assuming instantaneous current interruption at current zero and infinite post-interruption insulation strength. These simplifications leading to a conservative estimation of the TRV peak value. Such assumptions are consistent with IEC-based verification and ensure design robustness. Detailed time-domain simulations incorporating breaker-specific characteristics are required when accurate assessment of insulation margins and restrike risk is needed.

## 3 Calculation of the Voltage $u_l(t)$

After the fault current is interrupted from the network side, the portion of the system to the left of the circuit breaker can be represented by the equivalent circuit shown in Figure 2.

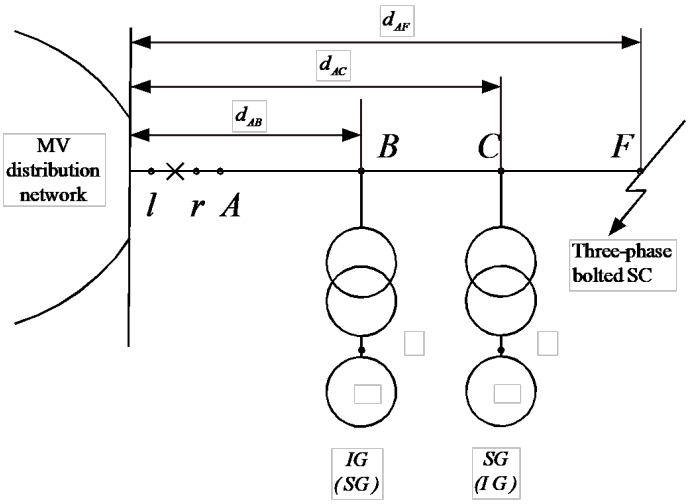


**Figure 1.** Diagram of the analyzed section of the electrical distribution system [20].

The current flowing toward the fault location, denoted as $i_{n,s}(t)$, can be calculated using eq. (2) [17–19]:

$$i_{n,s}(t) = \sqrt{2} \cdot \frac{U_{ns}}{\sqrt{3}} \frac{1}{Z_n} \cdot \sin(\omega_s \cdot t + \alpha_0 - \varphi_n) - \sqrt{2} \cdot \frac{U_{ns}}{\sqrt{3}} \frac{1}{Z_n} \cdot \sin(\alpha_0 - \varphi_n) \exp\left(-\frac{t}{T_n}\right) \tag{2}$$

and the voltage $u_l(t)$, according to [1], is obtained from

$$u_l(t) = \frac{\omega_i^2}{\omega_i^2 - \omega^2} \cdot \sqrt{2} \cdot \frac{U_{ns}}{\sqrt{3}} \cdot [\cos(\omega \cdot t) - \exp(-\delta \cdot t) \cdot \cos(\omega_i \cdot t)] \tag{3}$$

where

$$\delta = \frac{R_n}{2 \cdot L_n}, \quad \omega_i = \frac{1}{\sqrt{L_n \cdot C_l}} \tag{4}$$

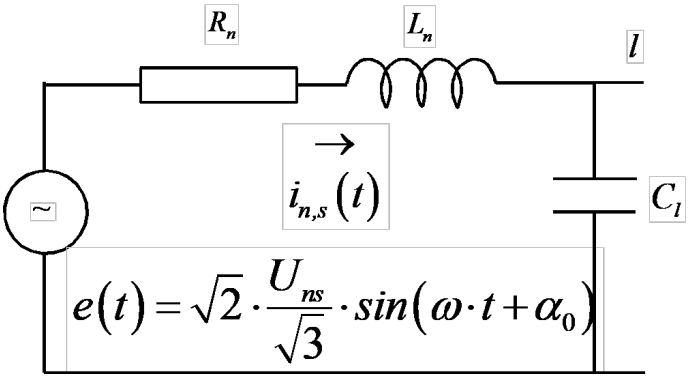


**Figure 2.** Equivalent network circuit for calculating the voltage $u_l(t)$.

## 4 Induction Generator Model

In the case of a three-phase short circuit at the generator terminals, a sufficiently accurate representation is obtained by using a voltage-source model in series with the transient direct-sequence impedance of the induction generator, as shown in Figure 3. In Figure 3:

$$V' = \left| U_{s,0} + \left(R_s + j \cdot X_s'\right) \cdot I_{s,0} \right| \tag{5}$$

where $U_{s,0}$ and $I_{s,0}$ denote the stator terminal voltage and the induction generator (IG) current prior to the fault occurrence, respectively.

The current flowing from the IG toward the fault location, denoted as $i_{IG,s}(t)$, is calculated from eq. (6) [17–19]:

$$i_{IG,s}(t) = \sqrt{2} \cdot \frac{U_{ns}}{\sqrt{3}\, Z_s'} \cdot \left[ \exp\left(-\frac{t}{T_s'}\right) \cdot \sin \alpha_0 - (1 - \sigma) \cdot \exp\left(-\frac{t}{T_r'}\right) \cdot \sin(\omega_s \cdot t + \alpha_0) \right] \tag{6}$$

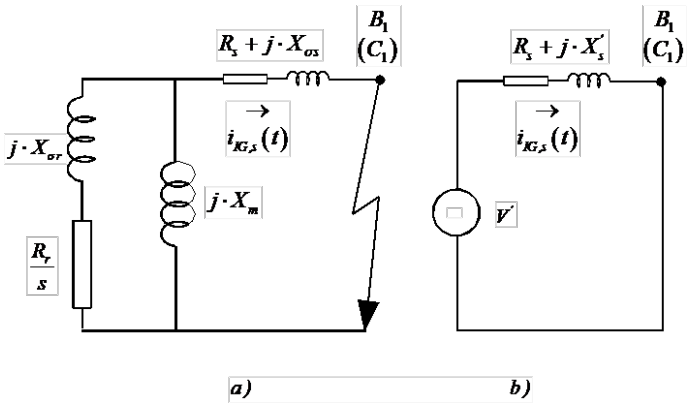


**Figure 3.** (a) Equivalent circuit of a squirrel-cage induction generator for determining the direct-sequence impedance. (b) Voltage-source model in series with the transient direct-sequence impedance of the IG.

## 5 Synchronous Generator Model

For the case of a bolted three-phase short circuit at the synchronous generator (SG) terminals, the current flowing from the SG toward the fault location, denoted as $i_{SG,s}(t)$, can be calculated using the following expression [17–19]:

$$i_{SG,s}(t) = -\sqrt{2} \cdot \frac{U_{ns}}{\sqrt{3}} \cdot \left(\frac{1}{Z_d''} - \frac{1}{Z_d''}\right) \cdot exp\left(-\frac{t}{T_d''}\right) \cdot cos\left(\omega_s \cdot t + \frac{\pi}{2} - \varphi_{SG}\right) - \sqrt{2} \cdot \frac{U_{ns}}{\sqrt{3}} \cdot \left[\left(\frac{1}{Z_d'} - \frac{1}{Z_d}\right) \cdot \exp\left(-\frac{t}{T_d'}\right) + \frac{1}{Z_d}\right] \cdot cos\left(\omega_s \cdot t + \frac{\pi}{2} - \varphi_{SG}\right) + \sqrt{2} \cdot \frac{U_{ns}}{\sqrt{3}} \cdot \frac{1}{Z_d''} \cdot \exp\left(-\frac{t}{T_a}\right) \cdot \sin \varphi_{SG} \tag{7}$$

Detailed comparative analysis between synchronous and induction machines for distributed generation applications is presented in [21].

## 6 Calculation of the Voltage $u_r(t)$

After the circuit breaker at point $A$ is opened, the currents flowing from the connected distributed generators toward the fault location are determined by applying the superposition theorem, as shown in [17–20]. Once the currents are obtained, the voltage at point $r$ is determined depending on which DG is closer to the given point, as illustrated in Figures 4 and 5.

By applying the procedure from [17–20], the currents flowing from the IG and SG toward the fault location are obtained as:

$$i_{IG}(t) = i_{IG,s}(t) + i_{SG-IG}(t) \tag{8}$$

$$i_{SG}(t) = i_{SG,s}(t) + i_{IG-SG}(t) \tag{9}$$

If the connection point of the IG is closer to point $r$, the voltage $u_r(t)$ is calculated according to:

$$u_r(t) = -L''_{SG,e} \cdot \frac{di_{SG}(t)}{dt} - R_{SG,e} \cdot i_{SG}(t) + \sqrt{2} \cdot \frac{U_{ns}}{\sqrt{3}} \cdot \sin(\omega_s \cdot t + \alpha_0) \tag{10}$$

and if the connection point of the SG is closer to point $r$, then:

$$u_r(t) = -L''_{SG,e} \cdot \frac{di_{SG}(t)}{dt} - R_{SG,e} \cdot i_{SG}(t) + \sqrt{2} \cdot \frac{U_{ns}}{\sqrt{3}} \cdot \sin(\omega_s \cdot t + \alpha_0) \tag{11}$$

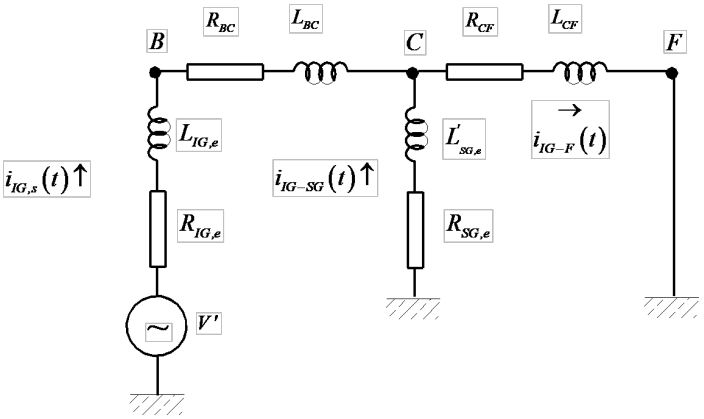


**Figure 4.** Diagram for determining the voltage $u_r(t)$ in the case where the IG is closer to point $r$.

## 7 Analyzed cases and input data for the calculation

By applying the previously described procedure, an analysis of the overvoltage coefficient

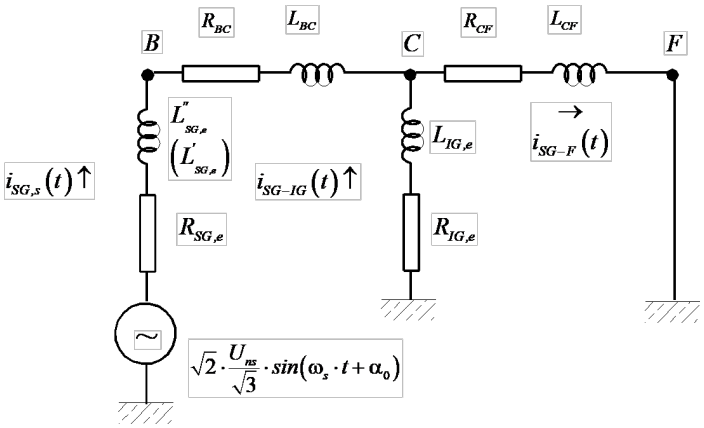


**Figure 5.** Diagram for determining the voltage $u_r(t)$ in the case where the SG is closer to point $r$.

$K_{lr} = max\left|\frac{u_{lr}(t)}{\sqrt{2}\cdot\frac{U_{ns}}{\sqrt{3}}} = \frac{u_l(t)-u_r(t)}{\sqrt{2}\cdot\frac{U_{ns}}{\sqrt{3}}}\right|$ will be performed, depending on whether and where DG units of a given type are connected to the feeder, as shown in Figure 1. The value of the voltage $u_l(t)$ does not depend on the configuration on the load side.

The value of the voltage $u_r(t)$ will be calculated for the following cases:

- One IG is connected to the feeder at one of the points $A, B, C$ or $F$. These cases are designated by the notation $E_{X-IG}$, $X = A, B, C, F$.
- One SG is connected to the feeder at one of the points $A, B, C$ or $F$. These cases are designated by the notation $E_{Y-SG}$, $Y = A, B, C, F$.
- One IG and one SG are connected to the feeder, with the IG being closer to the supply busbars than the SG. These cases are designated by the notation $E_{X-IG} - E_{Y-SG}$, with the following conditions:
  - If $X = A$, then $Y = B, C, F$;
  - If $X = B$, then $Y = C, F$;
  - If $X = C$, then $Y = F$.
- One SG and one IG are connected to the feeder, with the SG being closer to the supply busbars than the IG. These cases are designated by the notation $E_{Y-SG} - E_{X-IG}$, with the following conditions:
  - If $Y = A$, then $X = B, C, F$;
  - If $Y = B$, then $X = C, F$;
  - If $Y = C$, then $X = F$.

Therefore, the analysis will be performed for 20 connection scenarios, each evaluated for three

**Table 1.** Data on the case study that is defined by Figure 1.

| Component or initial conditions | Data |
|---|---|
| Radial MV feeder | • Feeder section lengths: $d_{AB} = 0.5$ km, $d_{AC} = 1$ km, and $d_{AF} = 1.5$ km<br>• Three single core cables with copper conductors, conductor cross-sectional area of 150 mm$^2$, and ampacity of 350 A<br>• Feeder series-resistance and series-inductance per unit length: $r_{\text{feeder}} = 0.12\ \Omega$/km, and $l_{\text{feeder}} = 0.32 \cdot 10^{-3}$ H/km |
| MV distribution network | • Rated voltage: $U_{n,N} = 10$ kV<br>• $S''_N = 250$ MVA, $T_{a,N} = 0.05$ s, $R_N = 0.025\ \Omega$, and $L_N = 1.27 \cdot 10^{-3}$ H |
| Induction generator | • Rated parameters: $S_{n,IG} = 2.5$ MVA, $U_{n,IG} = 0.69$ kV, $r_s = 0.004843$ p.u., $x_{\sigma s} = 0.1248$ p.u., $r_r = 0.004347$ p.u., $x_{\sigma r} = 0.1791$ p.u., and $x_m = 6.77$ p.u. |
| Induction generator step-up transformer | • Rated parameters: $m_{n,IGT} = 10/0.69$ kV/kV, $S_{n,IGT} = 4$ MVA, $r_{IGT} = 0.01$ p.u., and $x_{IGT} = 0.05$ p.u. |
| Synchronous generator | • Rated parameters: $S_{n,SG} = 2.5$ MVA, $U_{n,SG} = 0.48$ kV, $x''_d = 0.125$ p.u., $x'_d = 0.227$ p.u., $x_d = 3.064$ p.u., $T''_{d0} = 0.0132$ s, $T'_{d0} = 4.965$ s, and $T_{a,SG} = 0.0262$ s |
| Synchronous generator step-up transformer | • Rated parameters: $m_{n,SGT} = 10/0.48$ kV/kV, $S_{n,SGT} = 4$ MVA, $r_{SGT} = 0.01$ p.u., and $x_{SGT} = 0.05$ p.u. |
| Initial conditions | • It is assumed that the MV distribution network and two DGs were operating at no-load before the fault occurs |

current-interruption times $t_p$. Considering the characteristics of the relay protection system components, the first two values of $t_p$ are theoretical. The parameters required for the calculation are given in Table 1.

## 8 Calculation results

First, the most unfavorable instant of fault inception was determined, that is, the value of the angle $\alpha_0$. The component that exerts the greatest influence on equipment stress is the current $i_n(t)$ flowing from the grid. If the fault occurs at the instant $\alpha_0 = 0.84 \cdot \pi$ when current reaches its maximum value, the resulting stress will be the highest [20]. The overvoltage calculation was performed from the moment the current $i_n(t)$ was interrupted, i.e., at the instant $t_p$.

**Table 2.** Overvoltage coefficient values for the case when only the IG is connected to the feeder.

| | The analyzed case | | | |
|---|---|---|---|---|
| | $E_{A-IG}$ | $E_{B-IG}$ | $E_{C-IG}$ | $E_{F-IG}$ |
| $t_p[s]$ | The value of the overvoltage coefficient | | | |
| 0.01639 | 2.230 | 2.237 | 2.244 | 2.249 |
| 0.03581 | 2.202 | 2.206 | 2.211 | 2.215 |
| 0.05572 | 2.177 | 2.177 | 2.177 | 2.176 |

The calculation results are presented in Tables 2, 3, 4, and 5, based on which the following conclusions can be drawn:

**Table 3.** Overvoltage coefficient values for the case when only the SG is connected to the feeder.

| | The analyzed case | | | |
|---|---|---|---|---|
| | $E_{A-SG}$ | $E_{B-SG}$ | $E_{C-SG}$ | $E_{F-SG}$ |
| $t_p[s]$ | The value of the overvoltage coefficient | | | |
| 0.01639 | 2.501 | 2.509 | 2.517 | 2.526 |
| 0.03581 | 2.450 | 2.455 | 2.460 | 2.465 |
| 0.05572 | 2.422 | 2.426 | 2.431 | 2.435 |

- The overvoltage magnitude decreases as the interruption time $t_p$ of the current $i_n(t)$ increases;
- If only one DG unit (IG or SG) is connected to the feeder, the overvoltage coefficient increases with the distance of the generator interconnection point from the supply busbars. The overvoltage is higher when only the SG is connected to the feeder;
- If both types of generators are connected to the feeder, the overvoltage magnitude is lower compared to the case when only a single DG unit is connected;
- If both types of generators are connected to the feeder, the overvoltage magnitude is higher when the IG is closer to the supply busbars (and the SG is closer to the fault location).

**Table 4.** Overvoltage coefficient values for the case when both generator types are connected to the feeder, with the IG located closer to the supply busbars.

| | The analyzed case | | | | | |
|---|---|---|---|---|---|---|
| | $E_{A-IG} - E_{B-SG}$ | $E_{A-IG} - E_{C-SG}$ | $E_{A-IG} - E_{F-SG}$ | $E_{B-IG} - E_{C-SG}$ | $E_{B-IG} - E_{F-SG}$ | $E_{C-IG} - E_{F-SG}$ |
| $t_p[s]$ | The value of the overvoltage coefficient | | | | | |
| 0.01639 | 2.248 | 2.240 | 2.233 | 2.245 | 2.243 | 2.242 |
| 0.03581 | 2.220 | 2.208 | 2.203 | 2.211 | 2.207 | 2.212 |
| 0.05572 | 2.183 | 2.179 | 2.177 | 2.182 | 2.178 | 2.180 |

**Table 5.** Overvoltage coefficient values for the case when both generator types are connected to the feeder, with the SG located closer to the supply busbars.

| | The analyzed case | | | | | |
|---|---|---|---|---|---|---|
| | $E_{A-SG} - E_{B-IG}$ | $E_{A-SG} - E_{C-IG}$ | $E_{A-SG} - E_{F-IG}$ | $E_{B-SG} - E_{C-IG}$ | $E_{B-SG} - E_{F-IG}$ | $E_{C-SG} - E_{F-IG}$ |
| $t_p[s]$ | The value of the overvoltage coefficient | | | | | |
| 0.01639 | 2.083 | 2.081 | 2.079 | 2.083 | 2.082 | 2.084 |
| 0.03581 | 2.060 | 2.064 | 2.063 | 2.064 | 2.065 | 2.064 |
| 0.05572 | 2.055 | 2.056 | 2.055 | 2.058 | 2.052 | 2.054 |

Finally, Figures 6–9 show the time-domain variations of overvoltage for several of the analyzed scenarios. In Figures 6-9, the X-axis shows the time elapsed since the fault occurrence, expressed in calculation steps, and the Y-axis shows the values of the coefficient $K_{lr}$. In general, the remaining scenarios exhibit the same waveform shape, with differences only in amplitude. Based on these plots, the following conclusions can be drawn:

- The transient response is damped more rapidly when only the IG is connected to the feeder;
- If both DG types are connected to the feeder, the transient response is damped more rapidly when the IG is located closer to the supply busbars than the SG.

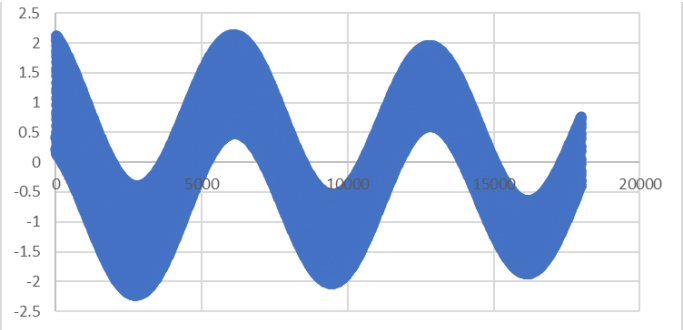


**Figure 6.** Time-domain variation of overvoltage for the case in which the IG is connected at point A (the calculation time step is $3\mu$s).

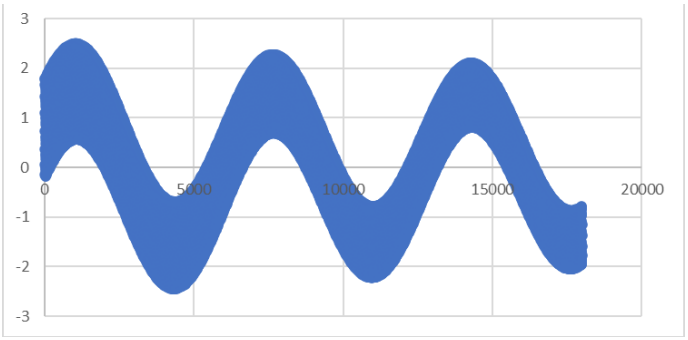


**Figure 7.** Time-domain variation of overvoltage for the case in which the SG is connected at point A (the calculation time step is $3\mu$s).

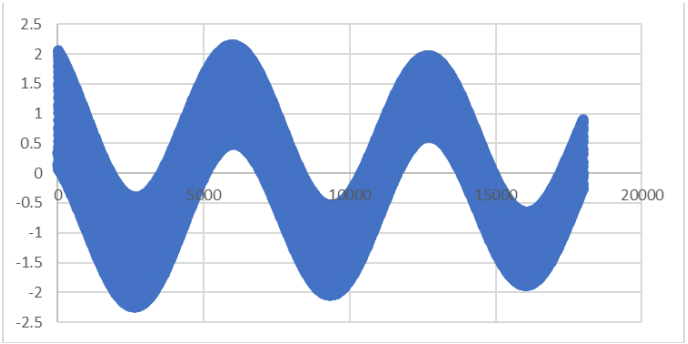


**Figure 8.** Time-domain variation of overvoltage for the case in which the IG is located closer to the supply busbars than the SG (the calculation time step is $3\mu$s).

## 9 Conclusion

This paper presents the procedure and results of calculating the switching overvoltage at the main circuit breaker of a medium-voltage cable feeder to which induction and/or synchronous generators are connected during a three-phase short circuit. The models of all system components are known. An analysis was carried out to assess the influence of the DG type and the generator interconnection point on the overvoltage magnitude. The results demonstrate the following:

- The overvoltage magnitude decreases as the

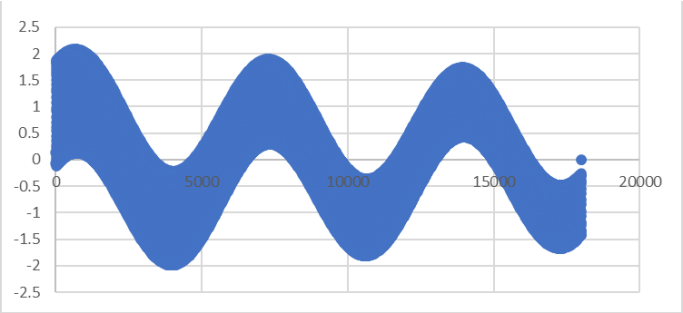


**Figure 9.** Time-domain variation of overvoltage for the case in which the SG is located closer to the supply busbars than the IG (the calculation time step is 3$\mu$s).

interruption time of current increases;

- If only one DG unit (IG or SG) is connected to the feeder, the overvoltage coefficient increases with the distance of the generator interconnection point from the supply busbars. The overvoltage is higher when only the SG is connected;
- If both types of generators are connected to the feeder, the resulting overvoltage is lower compared to the case when only a single DG unit is connected;
- If both types of generators are connected to the feeder, the overvoltage is higher when the IG is located closer to the supply busbars (and the SG is closer to the fault location);
- The transient response is damped more rapidly when only the IG is connected to the feeder;
- If both DG types are connected to the feeder, the transient response is damped more rapidly when the IG is located closer to the supply busbars than the SG.

Generally speaking, the shape of the presented graphs corresponds to that of the respective graphs in passive distribution networks. The oscillations that can be observed are a result of the different responses of the supplying network, synchronous generators, and induction generators to faults in the system.

In the available literature, we were unable to find studies that have analyzed a similar problem, and therefore we are unable to compare our results with those of other authors.

Research on switching overvoltages and transient processes in active distribution networks has increasingly focused on the impact of distributed energy resources and power electronic interfacing on network transient behavior. The presence of inverter-based generation significantly alters the magnitude, frequency content, and damping of switching transients compared to conventional passive electrical distribution networks. Particular attention is devoted to transient interactions between vacuum circuit breakers, cable feeders, and distributed generators, which may lead to fast overvoltages and increased insulation stress. Consequently, advanced electromagnetic transient modeling and insulation coordination approaches are required to ensure reliable operation of contemporary active distribution systems.

## Data Availability Statement

Data will be made available on request.

## Funding

This work was supported by the Ministry of Science, Technological Development and Innovation of the Republic of Serbia, and these results are parts of the Grant No. 451-03-136/2025-03/200132, with University of Kragujevac - Faculty of Technical Sciences Čačak.

## Conflicts of Interest

The authors declare no conflicts of interest.

## Ethical Approval and Consent to Participate

Not applicable.

## References

[1] Smeets, R., Van der Sluis, L., Kapetanovic, M., Peelo, D. F., & Janssen, A. (2015). *Switching in electrical transmission and distribution systems*. John Wiley & Sons. [Crossref]

[2] Emarati, M., Barani, M., Farahmand, H., Aghaei, J., & del Granado, P. C. (2021). A two-level over-voltage control strategy in distribution networks with high PV penetration. *International Journal of Electrical Power & Energy Systems, 130*, 106763. [Crossref]

[3] Astapov, V., Shabbir, N., Rosin, A., Kütt, L., Maask, V., & Tiismus, H. (2025). Review of technical solutions addressing voltage and operational challenges in a distribution grid with high penetration of intermittent RES. *Energy Reports, 14*, 1738-1760. [Crossref]

[4] Adhikari, P. M., Vanfretti, L., Banjac, A., Bründlinger, R., Ruppert, M., & Ropp, M. (2023). Analysis of transient overvoltages and Self Protection Overvoltage of PV inverters through RT-CHIL. *Electric Power Systems Research, 214*, 108826. [Crossref]

[5] Chang, Y., Hou, W., Xu, G., Hong, H., & Zeng, X. (2023, December). An overvoltage adjustment strategy Based on Integrated Voltage Sensitivity in the Active Distribution Network. In *Journal of Physics: Conference Series* (Vol. 2662, No. 1, p. 012014). IOP Publishing. [Crossref]

[6] Avilés, J., Guillen, D., Ibarra, L., & Dávalos-Soto, J. D. (2024). Reconfiguration of active distribution networks as a means to address generation and consumption dynamic variability. *IET Generation, Transmission & Distribution, 18*(19), 3120-3137. [Crossref]

[7] Akinyemi, A. S., Musasa, K., & Davidson, I. E. (2022). Analysis of voltage rise phenomena in electrical power network with high concentration of renewable distributed generations. *Scientific Reports, 12*(1), 7815. [Crossref]

[8] Guillén-López, D., Serrano-Guerrero, X., Barragán-Escandón, A., & Clairand, J. M. (2024). Transient and Steady-State Evaluation of Distributed Generation in Medium-Voltage Distribution Networks. *Energies, 17*(22), 5783. [Crossref]

[9] Chen, L., Zhang, X., Chen, H., Li, G., Yang, J., Tian, X., ... & Tang, Y. (2019). Pareto optimal allocation of resistive-type fault current limiters in active distribution networks with inverter-interfaced and synchronous distributed generators. *Energy Science & Engineering, 7*(6), 2554-2571. [Crossref]

[10] El-Ela, A. A. A., El-Sehiemy, R. A., Shaheen, A. M., & Ellien, A. R. (2022). Review on active distribution networks with fault current limiters and renewable energy resources. *Energies, 15*(20), 7648. [Crossref]

[11] Alam, M. S., Abido, M. A. Y., & El-Amin, I. (2018). Fault current limiters in power systems: A comprehensive review. *Energies, 11*(5), 1025. [Crossref]

[12] Zayed, M. S., Attia, H. E., Emara, M. M., Mansour, D. E. A., & Abdelfattah, H. (2025). Development of a New Solid State Fault Current Limiter for Effective Fault Current Limitation in Wind-Integrated Grids. *Electronics, 14*(20), 4054. [Crossref]

[13] Dehghani-Ashkezari, M., Modaresi, S. M., Saied, S., Daemi, T., & Akbari, H. (2024). Impact of inductive and resistive fault current limiters for transient stability Improvement based on difference between accelerating and decelerating areas. *Heliyon, 10*(16). [Crossref]

[14] Ahmed, A. R., Hamada, A. M., Hasan, S., & Abdel-Latif, K. M. (2024). Inexpensive short-circuit current limiter and switching device based on one commutation circuit for a three-phase system. *Journal of Electrical Systems and Information Technology, 11*(1), 6. [Crossref]

[15] Fard, A. K., Wang, B., Avatefipour, O., Dabbaghjamanesh, M., Sahba, R., & Sahba, A. (2019, June). Superconducting fault current limiter allocation in reconfigurable smart grids. In *2019 3rd International Conference on Smart Grid and Smart Cities (ICSGSC)* (pp. 76-80). IEEE. [Crossref]

[16] Bayati, N., Sadeghi, S. H. H., & Hosseini, A. (2017). Optimal placement and sizing of fault current limiters in distributed generation systems using a hybrid genetic algorithm. *Engineering, Technology & Applied Science Research, 7*(1), 1329-1333. [Crossref]

[17] Karaliolios, P., Ishchenko, A., Coster, E., Myrzik, J., & Kling, W. (2008, September). Overview of short-circuit contribution of various distributed generators on the distribution network. In *2008 43rd international universities power engineering conference* (pp. 1-6). IEEE. [Crossref]

[18] Tleis, N. (2007). *Power systems modelling and fault analysis: theory and practice*. Elsevier. [Crossref]

[19] Howard, D. F., Restrepo, J., Smith, T., Starke, M., Dang, J., & Harley, R. G. (2011, July). Calculation of fault current contribution of Type I wind turbine-generators. In *2011 IEEE power and energy society general meeting* (pp. 1-7). IEEE. [Crossref]

[20] Mijailović, V., Klimenta, D., Ranković, A., Petrović, P., & Milovanović, M. (2024). Calculation of three-phase bolted short-circuit currents in a MV distribution feeder with induction and synchronous generators. *Electrical Engineering, 106*(1), 459-473. [Crossref]

[21] Freitas, W., Vieira, J. C., Morelato, A., Da Silva, L. C., Da Costa, V. F., & Lemos, F. A. (2006). Comparative analysis between synchronous and induction machines for distributed generation applications. *IEEE transactions on Power Systems, 21*(1), 301-311. [Crossref]

## Appendix: The application of the theorem of superposition [20]

The theorem of superposition states that in any linear circuit having more than one input (voltage or current source), the response (voltage across or current through a component) to a sum of inputs is the sum of the responses (voltages across or currents through that component) to each input applied separately. In particular, this means that the contributions of each source (MV distribution network, IG or SG) to the instantaneous output currents should be calculated separately under the assumption that all remaining sources are short-circuited.

The theorem of superposition will be applied to the case study defined by Figure 1, that is, the radial MV feeder with one IG at the point B, one SG at the point C, and the three-phase bolted SC at the point F. According to the theory and Figure 1, there are three inputs, independent current sources (MV distribution network, IG, and SG),

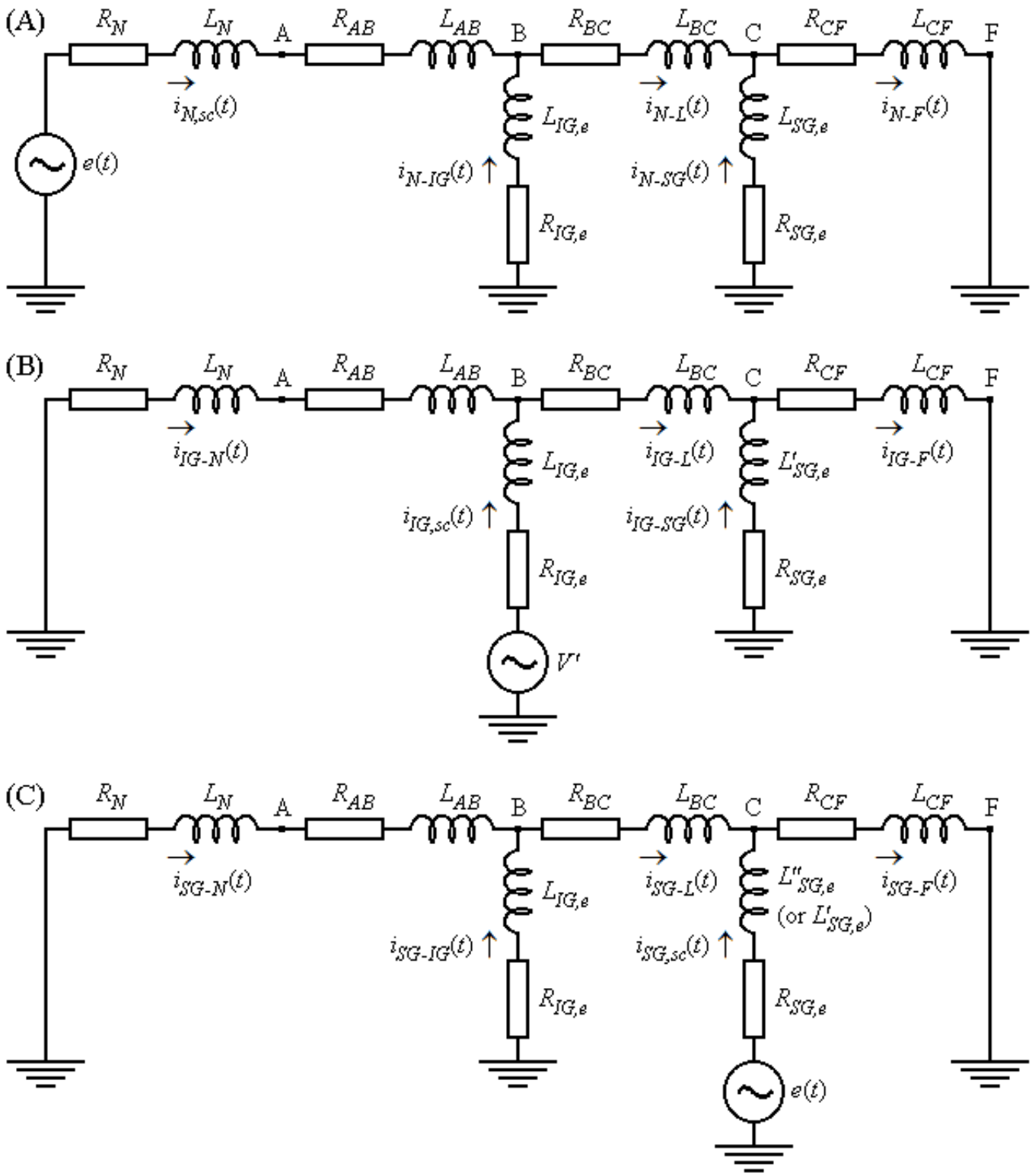


**Figure A1.** Equivalent circuits of the case study under consideration in the case when A, MV distribution network, B, IG, C, SG acts alone, while the two remaining sources are short-circuited.

and five outputs, the instantaneous output currents $i_N(t), i_{IG}(t), i_L(t), i_{SG}(t)$, and $i_F(t)$ in kA. Accordingly, the contributions of each input to the outputs are calculated separately under the assumption that all remaining inputs are short-circuited. Figure A1 illustrates the case when the MV distribution network acts alone with the IG and SG are replaced by short-circuits. Figure A1(B) corresponds to the case when the IG acts alone, while Figure A1(C) corresponds to the case when the SG acts alone.

**Vladica Mijailović** was born in Serbia in 1966. He graduated from the Faculty of Electrical Engineering, University of Belgrade, in 1991. Also, he received his postgraduate M.Sc. and Ph.D. in 1995. and 1999, respectively, from the Faculty of Electrical Engineering, University of Belgrade. His main research interests include Reliability of electrical distribution systems, Monitoring and diagnostics of HV switchgears components and Renewable power resources. Currently, he is a full professor Faculty of Technical Sciences in Cacak, University of Kragujevac. (Email: vladica.mijailovic@ftn.kg.ac.rs)

**Aleksandar Ranković** was born in Serbia in 1971. He received the B.Sc. degree from Technical Faculty Cacak, University of Kragujevac, Republic of Serbia in 1994. and M.Sc., and Ph.D. degrees in electrical engineering from the University of Belgrade, Belgrade, Republic of Serbia, in 2002 and 2010, respectively. His main areas of interest are Power system analysis and Electromagnetic compatibility. At present he is a full professor Faculty of Technical Sciences in Cacak, University of Kragujevac. (Email: aleksandar.rankovic@ftn.kg.ac.rs)